ACS Infectious Diseases

Article

pubs.acs.org/journal/aidcbc

Bacterial Transcription Inhibitor of RNA Polymerase Holoenzyme Formation by Structure-Based Drug Design: From in Silico Screening to Validation

Cong Ma, Xiao Yang, and Peter J. Lewis*

School of Environmental and Life Sciences, University of Newcastle, Callaghan, New South Wales 2308, Australia

Supporting Information

ABSTRACT: Bacterial transcription is a proven target for antibacterial research. However, most of the known inhibitors targeting transcription are from natural extracts or are hits from screens where the binding site remains unidentified. Using an RNA polymerase holoenzyme homology structure from the model Gram-positive organism *Bacillus subtilis*, we created a pharmacophore model and used it for in silico screening of a publicly available library for compounds able to inhibit holoenzyme formation. The hits demonstrated specific affinity to bacterial RNA polymerase and excellent activity using in vitro assays and showed no binding to the equivalent structure from human RNA polymerase II. The target specificity in live cells and antibacterial activity was demonstrated in microscopy and growth inhibition experiments. This is the first example of targeted inhibitor development for a bacterial RNA polymerase, outlining a complete discovery process from virtual screening to biochemical validation. This approach could serve as an appropriate platform for the future identification of inhibitors of bacterial transcription.

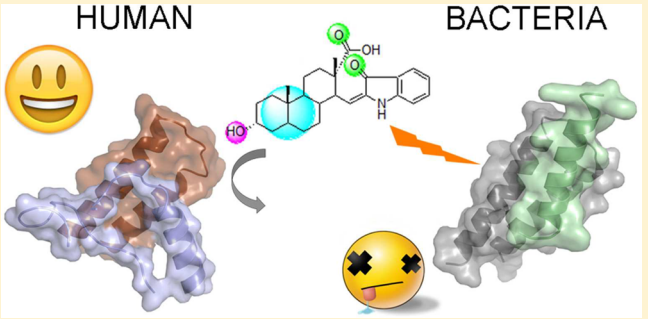

KEYWORDS: *transcription, bacteria, protein−protein interaction, antibiotic discovery, in silico screening, target validation*

Bacterial infection is a global health problem responsible for numerous deadly and debilitating diseases such as pneumonia, tuberculosis, and many gastrointestinal diseases including peptic ulcers, which cost health systems billions of dollars annually worldwide.[1] They are projected to cause >10 million deaths per year (more than the current annual number of deaths due to cancer) and cost the global economy U.S. $100 trillion per year by 2050 if no new efficient drugs are developed.[2] Transcription, together with DNA replication and protein translation, is an essential step in the bacterial cell cycle, which requires RNA polymerase (RNAP) as the core enzyme along with a suite of transcription factors to convert DNA sequences into RNA containing the same genetic information.[3] The discovery and development of rifampicin in the 1950s established bacterial transcription as a valid target for antibiotic development.[4] Despite the subsequent identification of many further inhibitors of transcription, only fidaxomicin, in 2011, has successfully gained approval for clinical use as a narrow-spectrum drug for the treatment of *Clostridium difficile*-associated diarrhea.[5] So far, most of the transcription inhibitors reported have been natural products with complex structures requiring arduous fermentation and extraction procedures.[6] Furthermore, as they tend to bind at or near the active site of RNAP in a large cleft comprising a substantial surface area made from the two large subunits (β and β'), point mutations at multiple sites have led to rapid acquisition of resistance, which has prevented their development as clinically useful drugs.[7] Resistance to rifampicin occurs so rapidly it is used only in combination therapy, and resistance to fidaxomicin was first reported ∼40 years ago.[8]

The initiation of transcription requires RNAP holoenzyme, which is formed by association of the RNAP core enzyme ($\alpha_2\beta\beta'\omega$ and ε in the Gram-positive firmicutes) with an essential σ factor (Figure 1A,B; σ^A in *Bacillus subtilis*) required for specific recognition of promoter DNA sequences.[9,10] Therefore, compounds that prevent holoenzyme formation should be able to inhibit bacterial transcription and could potentially be developed as antibacterials. The SB series of compounds was shown to inhibit RNAP holoenzyme formation,[11] and anthralinic acid derivatives identified by virtual screening of a pharmacophore model based on alignment to the SB series and other compounds with unknown or diverse binding sites on RNAP were recently reported to display activity against holoenzyme formation and transcription by in vitro binding and functional assays.[12] However, the exact binding sites of these compounds are still unknown.

Although σ^A makes extensive contacts with the RNAP core, it is the interaction between α-helices in the β' subunit clamp−helix (β'-CH) region and σ region 2.2 ($\sigma_{2.2}$) that is absolutely necessary for the formation of holoenzyme.[13,14] An incomplete

Received: May 5, 2015
Published: September 21, 2015

DOI: 10.1021/acsinfecdis.5b00058
ACS Infect. Dis. 2016, 2, 39−46

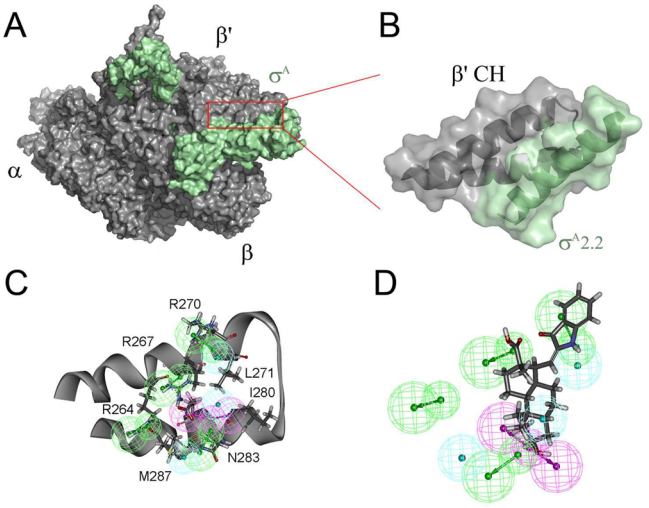

Figure 1. (A) Homology model of *B. subtilis* RNAP HE. RNAP core subunits are shown in gray and σ^A in pale green. (B) Expanded view of the interaction between RNAP and σ^A showing the β' CH region and $\sigma_{2.2}$ regions. (C) New pharmacophore model utilizing mutagenesis data overlaid on the β' CH region with hydrogen bond acceptors in green, hydrophobic interactions in cyan, and hydrogen bond donors in magenta. (D) Compound **C5** fitting to the pharmacophore model.

pharmacophore designed to target this interaction has been used to identify compounds that inhibit bacterial transcription in vitro and in vivo with some success.[14,15] Past studies have also identified inhibitors from natural product extracts using a high-throughput screen, but these have not been developed further.[16,17] To generate bona fide lead molecules it has been necessary to more comprehensively characterize the $\sigma_{2.2}$–β'-CH interaction to enable construction of a fully effective pharmacophore. The studies outlined in this work established a more comprehensive pharmacophore model based on in silico modeling and biochemical verification and allowed rational high-throughput identification of highly specific new lead compounds from a public drug-like compound library[18] for potential development as a novel class of antibiotic.

RESULTS AND DISCUSSION

In previous studies a pharmacophore model was built incorporating *B. subtilis* σ^A mutagenesis data obtained from far-Western blots.[14,15] However, an ELISA-based affinity assay of mutant β'-CH with σ^A identified additional interactions that could be used for optimal pharmacophore model construction.[14] Therefore, an improved pharmacophore model was created (Figure 1C,D) incorporating all available data and with the following properties: (1) Hit compounds had to map to the region representing β'-CH residue R267 (Figure 1C) as this is the most important residue required for interaction with σ^A.[14] (2) Considering that the binding site of β'-CH to σ^A is nearly a flat surface rather than a pocket, exclusion regions present in the original pharmacophore[14] were deleted to allow for more flexible conformational changes of inhibitor compounds. (3) Hit compounds could fit in the region representing residue R264 as binding studies showed that it was important in the β'-CH–σ^A interaction.[14]

Using this improved pharmacophore, we undertook the identification of a drug lead with good solubility and appropriate drug-like properties[18] through in silico screening of publicly available compound libraries. After screening the mini-Maybridge library (53000 compounds; http://www.maybridge.com/), 27 hits were identified, from which 7 that demonstrated the appropriate distance constraints to the β'-CH region and energy-minimized conformations were short-listed for further investigation (Figure 2). Figure 1D shows one of the compounds from the seven selected hits (compound **C5**; Maybridge no. DSHS00507), fitted into the pharmacophore model.

All seven compounds were initially tested in an ELISA-based binding assay using σ^A and a GST-tagged β' subunit fragment that encompasses the CH region (β'-CH).[14] Three of the seven compounds possessed inhibitory activity against the binding of σ^A and β' fragments (Figure 3A). Compounds **C3**–**C5** all

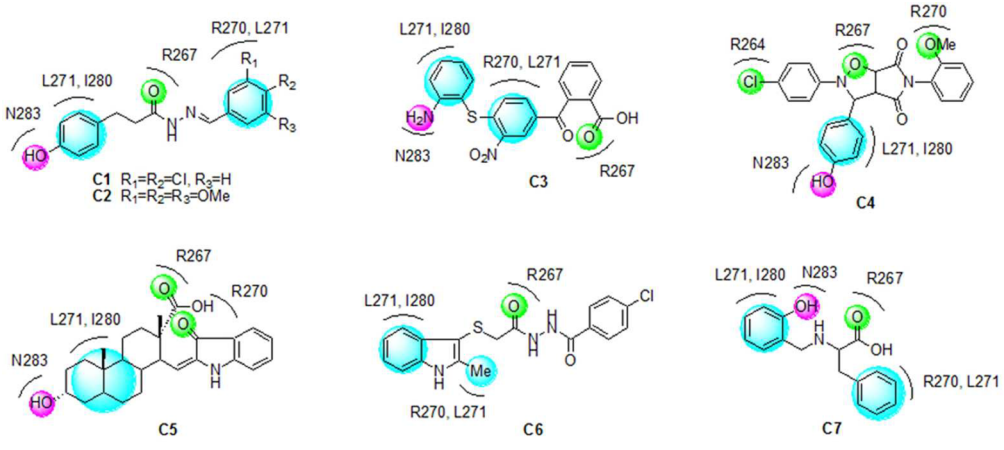

Figure 2. Seven hits, labeled **C1**–**C7**, identified from the in silico screen of the mini-Maybridge library. Purple sphere, hydrogen bond donor; green sphere, hydrogen bond acceptor; cyan sphere, hydrophobic interaction. **C1**, *N*′-[(1*E*)-(3,4-dichlorophenyl)methylidene]-3-(4-hydroxyphenyl)-propanehydrazide (Maybridge no. BTB01033); **C2**, 3-(4-hydroxyphenyl)-*N*′-[(1*E*)-(3,4,5-trimethoxyphenyl)methylidene]propanehydrazide (Maybridge no. BTB01034); **C3**, 2-{4-[(2-aminophenyl)sulfanyl]-3-nitrobenzoyl}benzoic acid (Maybridge no. BTB02887); **C4**, 2-(4-chlorophenyl)-3-(4-hydroxyphenyl)-5-(2-methoxyphenyl)-hexahydro-2*H*-pyrrolo[3,4-*d*][1,2]oxazole-4,6-dione (Maybridge no. BTB14348); **C5**, (2*S*,4b*S*,7*R*)-7-hydroxy-2,4*b*-dimethyl-1-{[(2*E*)-3-oxo-1*H*-indol-2-ylidene]methyl}dodecahydrophenanthrene-2-carboxylic acid (Maybridge no. DSHS00507); **C6**, 4-chloro-*N*′-{2-[(2-methyl-1*H*-indol-3-yl)sulfanyl]acetyl}benzohydrazide (Maybridge no. KM07812); **C7**, 2-{[(2-hydroxyphenyl)methyl]amino}-3-phenylpropanoic acid (Maybridge no. RH00596).

DOI: 10.1021/acsinfecdis.5b00058
ACS Infect. Dis. 2016, 2, 39–46

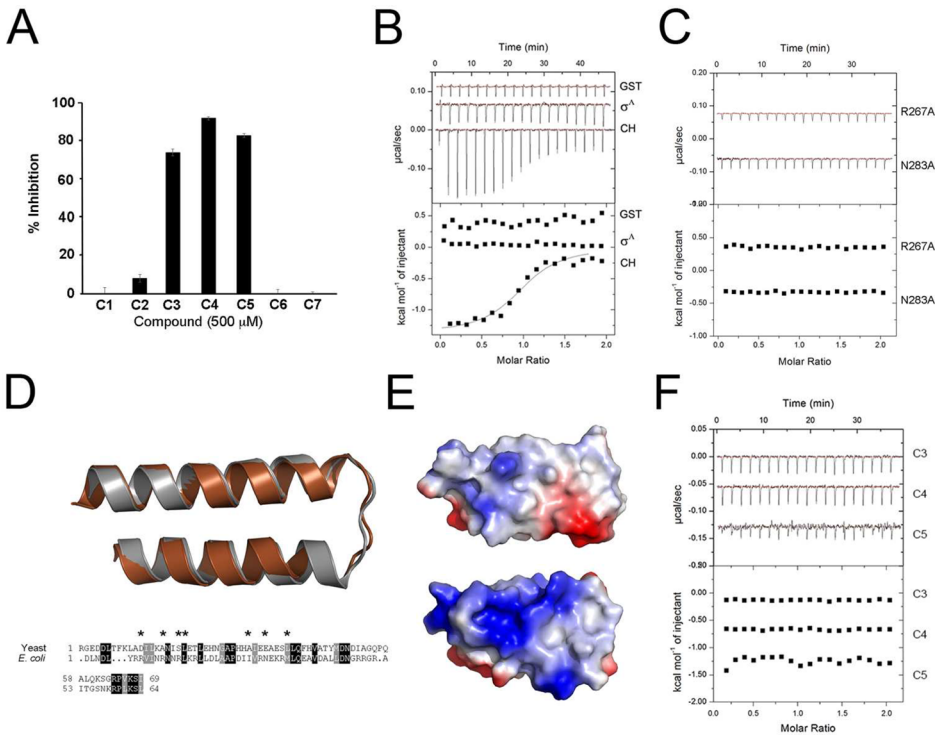

Figure 3. (A) Assay of hit compound activity determined by ELISA of the β'-CH–σ^A interaction. Inhibitor compounds were used at 500 μM. (B) ITC titration of compound **C5** against GST-tagged β'-CH, σ^A, and free GST. (C) Titration of **C5** against GST-tagged β'-CH with R267A and N283A substitutions, respectively. (D) Comparison of CH motifs from *S. cerevisiae* (brown, PDB ID 3K1F) and *E. coli* (gray, PDB ID 4IGC). Sequence alignments are shown below with identical residues highlighted in black and similar residues in gray. Asterisks above the alignment indicate amino acids determined from previous studies to be important for interaction with σ. (E) Surface electrostatic representations of *S. cerevisiae* (top) and *E. coli* (bottom) CH motifs. White, hydrophobic; red, acidic; blue, basic. (F) ITC titration of compounds **C3**–**C5** against GST-tagged human RPB1 CH.

showed good inhibitory activity at the high concentration used (500 μM), but only **C5** displayed significant activity at lower concentrations. Therefore, further studies concentrated on **C5**. Previously, we demonstrated that σ^A bound to a β'-CH–GST fusion protein in a 1:1 ratio with a $K_d \sim 1$ μM by isothermal titration calorimetry (ITC).[14] In similar experiments, **C5** bound specifically to the β'-CH–GST fusion (Figure 3B), with a K_d = 3.10 ± 0.99 μM with a one-site binding mode (N = 0.986 ± 0.037), ΔH = 1366 ± 70.65 cal/mol, and ΔS = 20.4 cal/mol/deg. No nonspecific binding was detected to free GST or σ^A proteins (Figure 3B). Titrations using β'-CH constructs where amino acids known to be required for interaction with σ^A were altered to alanine showed no significant binding to **C5** (Figure 3C).

Eukaryotic RNA polymerases contain a CH structure similar to the β'-CH but with no sequence similarity (Figure 3D), and in RPB1 of RNA polII, it is involved in binding to initiation factor TFIIB.[19] Alignment of the amino acid backbones from protein crystal structures of the CH regions from *Escherichia coli* RNAP and *Saccharomyces cerevisiae* RNA polII (gray and brown, respectively, Figure 3D) gave a root-mean-square deviation of ~0.9 Å, illustrating how similar these two structures are. However, examination of the surface charge indicated that the electrostatic environments of these two protein interaction interfaces were very different, with the eukaryotic CH region being relatively hydrophobic (white-gray, Figure 3E, top) and the bacterial CH region being dominated by basic side chains (blue, Figure 3E, bottom). Therefore, despite the similarity in structure, it should still be possible to identify compounds that will selectively bind to the bacterial CH region. To this end, we also examined whether compounds **C3**–**C5** could bind to a human RPB1 CH-containing fragment. No interaction between human RPB1 CH and compounds **C3**–**C5** could be detected by ITC (Figure 3F). These results demonstrate that **C5** targets the interaction between σ^A and β'-CH with a high level of specificity, laying the foundation for future elaboration of a compound with specific antibacterial activity.

The mechanism of transcription inhibition by **C5** was tested using in vitro transcription assays with *Escherichia coli* RNAP and its cognate essential σ factor, σ^{70}. Initially, **C5** was premixed with RNAP followed by the addition of σ^{70}. As shown in Figure 4A, the inhibitory activity positively correlated to the concentration of **C5**, and the IC_{50} was determined to be ~0.05 μM. This value was substantially lower than the K_d (~3 μM; Figure 3B), but it is important to bear in mind that the K_d was determined using a CH-containing fragment of RNAP, whereas the IC_{50} was determined from transcription assays with whole RNAP. It is possible that other regions of RNAP closely juxtaposed to the CH region, or differences in buffer composition, could influence **C5** binding in the transcription assays.

When performing these assays, we noticed that even at the highest concentration of **C5** (20 μM) it was not possible to obtain 100% inhibition of transcription (Figure 4A). The reason for this is unclear, although it was possible that **C5** was aggregating at high concentrations, leading to this effect. We found no evidence of aggregation by analysis of **C5** at 20 μM in transcription assay buffer by dynamic light scattering (data not shown). We believe it was possible that in these multiround

DOI: 10.1021/acsinfecdis.5b00058
ACS Infect. Dis. 2016, 2, 39–46

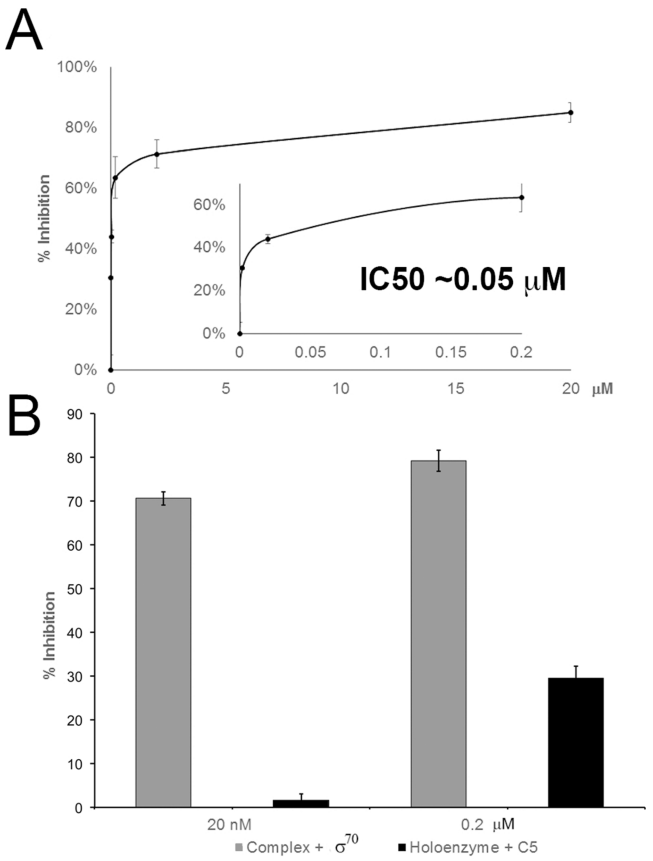

Figure 4. (A) Determination of the inhibition constant IC_{50} of *E. coli* RNAP transcription by compound **C5** in a multiround in vitro transcription assay. Percent inhibition of transcription was determined from the amount of product band produced on a transcription gel from a multiround assay and was plotted against concentration of **C5** (μM). (Inset) Expanded view of the curve from 0 to 0.2 μM compound **C5**. (B) Inhibitory activity of compound **C5** in single-round transcription assays when it was added before (complex + σ^{70}; gray) and after (Holoenzyme + **C5**; black) holoenzyme formation. In both panels plots are averages of triplicate experiments with standard deviations shown.

assays some σ^{70} was able to reassociate with RNAP, resulting in low-level transcription even at high concentrations of **C5**.

We also performed single-round transcription assays to determine whether **C5** was able to displace σ^{70} from RNAP. **C5** effectively inhibited transcription when added prior to σ^{70} (Figure 4B, gray columns), but was not able to efficiently displace σ^{70} already bound to RNAP (Figure 4B, black columns). Therefore, **C5** competes with σ^{70} for binding to the CH region to inhibit transcription, but is not able to displace σ^{70} that is already bound to RNAP, consistent with the ITC data where σ^{70} has ~3 times greater affinity for the CH than **C5**. Because σ^{70} is known to cycle on and off RNAP in vitro and in vivo,[20] we expected **C5** to have the ability to inhibit transcription in live cells.

When compound **C5** was used in bacterial growth inhibition assays, it displayed superior inhibitory activity against Gram-positive over Gram-negative bacteria (Figure 5). Growth was significantly affected at 12.5 μM in *B. subtilis* and at >50 μM in the community-acquired methicillin-resistant *Staphylococcus aureus* (CA-MRSA) strain USA300 (Figure 5A,B). The pattern of growth inhibition indicates the MIC value for *B. subtilis* was ≤50 μM and ~100 μM for CA-MRSA. We attribute the low activity of **C5** against Gram-negative bacteria (Figure 5C) to the presence of the impermeable outer membrane of these organisms, because it worked well against purified *E. coli* RNAP in the in vitro transcription assay (see Figure 4). **C5** did not show any inhibitory activity against *Saccharomyces cerevisiae* grown under similar conditions at levels of **C5** an order of magnitude greater than those used to inhibit bacterial growth (Figure 5D), supporting the ITC data with the human RPB1-CH fragment shown in Figure 3, which indicated the compound was specific against prokaryotes.

Epifluorescence microscopy was used to establish the compound's mechanism of action in live bacterial cells using two *B. subtilis* strains. BS23 contains a GFP fusion to the α subunit of the membrane-localized ATP synthase,[21] whereas BS1048 contains a GFP fusion to the β' subunit of RNAP that localizes to the central chromosome-containing lumen of the cell.[22] As shown in Figure 6, unlike the membrane-targeting compound colistin (Col) that causes readily detectable membrane damage (top middle), **C5** used at its MIC did not affect ATP synthase localization patterns (compare top left, control, with top right, + **C5**), indicating it does not affect bacterial membrane integrity, and the lack of change in cell shape (e.g., swelling, distortion) also indicates cell wall integrity is not affected. In contrast, RNAP-GFP localization in rifampicin (Rif) and **C5**-treated cells was very similar with chromosomes becoming elongated and decondensed compared to the control cells (Figure 6, bottom left, arrow showing nucleoid). Mechanistically, rifampicin inhibits transcription initiation through binding to the active site of RNAP, and this leads to loss of supercoiling in DNA and decondensed chromosomes.[23] Following **C5** treatment, chromosomes decondensed (as judged by localization of the RNAP−GFP fusion), similar to that seen on rifampicin treatment. However, aggregation of the GFP signal was also visible, which may possibly be a result of chromosome fragmentation prior to cell death. As an additional control, the effect of colistin on RNAP−GFP localization was also tested (bottom right panel, Figure 6). No effect on RNAP localization could be observed, and cell morphology as judged by phase contrast microscopy (top right panel) also appeared normal under these conditions. In summary, these results are consistent with **C5** targeting the transcription apparatus in live cells, resulting in a phenotype broadly similar to that observed on rifampicin treatment.

In this work we have identified a compound from an in silico screen of a commercial database (Maybridge) that specifically inhibits the interaction between bacterial RNAP and the major housekeeping σ factor. Although the structural motif targeted (the CH region) is conserved in eukaryotic RNAPs, in vitro (Figure 3) and live cell assays (Figure 5) show that the compound has no overlapping activity against eukaryotic RNAPs. The MIC values for **C5** against Gram-positive bacteria (50−100 μM, Figure 5A,B) are equivalent to ~20−40 μg/mL **C5**, which is within the concentration range used for compounds such as the β-lactams and is encouraging for a "first-pass" small-scale structure-based screen. The results of the fluorescence microscopy experiments (Figure 6) are consistent with this conclusion and that **C5** is targeting transcription in live cells as there was no perturbation of membrane integrity (as judged by the distribution of ATP synthase) but RNAP distribution was similar to that of rifampicin-treated cells.

Antibiotic development through modification of existing drugs is hampered by the spread of existing resistance mechanisms that often are also effective against these

DOI: 10.1021/acsinfecdis.5b00058
ACS Infect. Dis. 2016, 2, 39−46

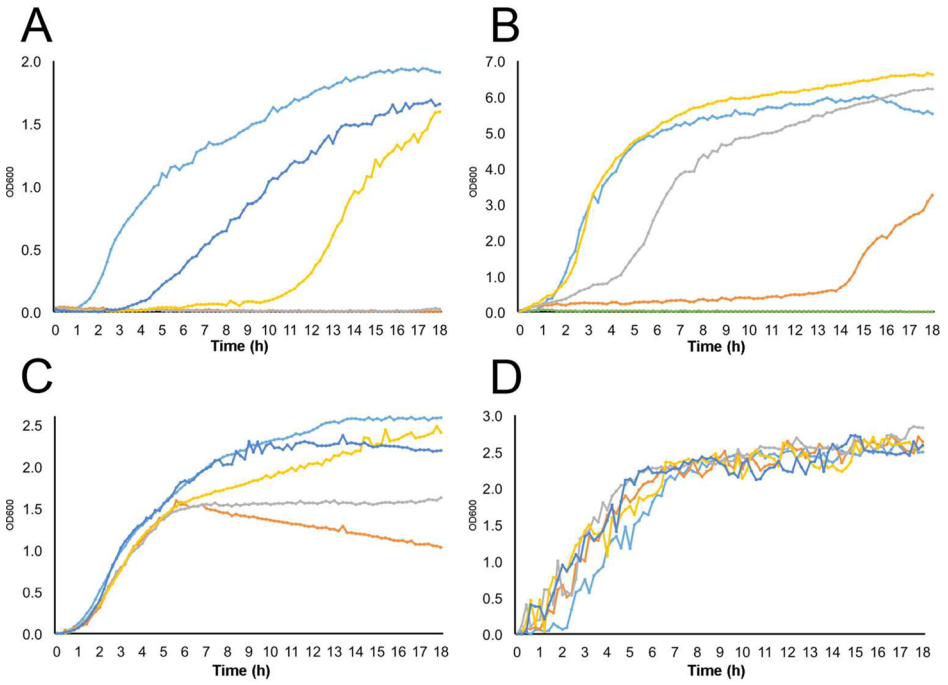

Figure 5. Antibacterial activity of compound **C5** against (A) *B. subtilis* strain 168, (B) *S. aureus* CA-MRSA strain USA300, and (C) *E. coli* DH5α. Light blue, control (no compound); dark blue, 12.5 μM **C5**; yellow, 25 μM **C5**; gray, 50 μM **C5**; orange, 100 μM **C5**; green, 200 μM (B only) **C5**. (D) *S. cerevisiae*. Light blue, control (no compound); dark blue, 125 μM **C5**; yellow, 250 μM **C5**; gray, 500 μM **C5**; orange, 1000 μM **C5**. All plots are averages of triplicates.

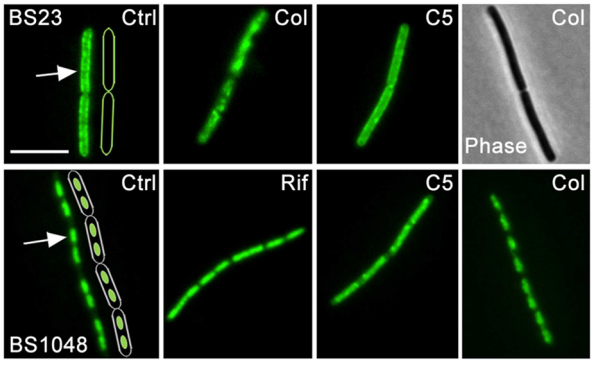

Figure 6. Fluorescence images of *B. subtilis* strain BS23 (GFP fusion to ATP synthase, top) and BS1048 (GFP fusion to RNAP, bottom). Ctrl, control; Col, colistin; Rif, rifampicin. Cartoon schematics are shown next to cells in the control panel illustrating GFP localization (green) and cell outline (white). Arrows indicate ATP synthase localization to the cell membrane (top) and RNAP localization to the nucleoid (bottom). The phase contrast image of colistin-treated BS1048 is shown in the top right panel. Scale bar = 4 μm.

derivatized compounds.[24] New classes of antibiotic are needed to increase the arsenal of drugs available to clinicians to effectively treat infections. By targeting the binding surface between RNAP and a transcription factor essential for cell viability, we have developed pharmacophore models rationally designed on the basis of protein structure and mutagenesis data. The refined in silico screen provided small molecules that were highly specific for the CH region of bacterial RNAP, with no evidence that they were able to target the equivalent structure of eukaryotic RNAPs and that showed no inhibitory activity to the growth of *S. cerevisiae* cultures at concentrations as high as 1 mM. Compound **C5** could inhibit transcription initiation in in vitro transcription assays and demonstrated antibacterial activity. Most importantly, **C5** exhibited the ability to inhibit the growth of the antibiotic-resistant strain CA-MRSA USA300. Together with **C3** and **C4**, the diverse structures of these compounds will help in the study and optimization of the structure−activity relationship potential for further development of drug leads. Furthermore, the high hit rate (27 hits, 7 short-listed, 3 with activity) from a public compound library demonstrated that this high-throughput in silico screening method using a carefully constructed and experimentally verified pharmacophore model will provide a solid platform for drug development targeting essential protein−protein interactions.

Bacterial transcription is a valid but under-developed target for antibiotic discovery. Here, we demonstrated the feasibility of structure-based design and validation for the discovery of transcription inhibitors. This platform, utilizing high-throughput virtual screening followed by biochemical confirmation of a small number of carefully chosen hits, may represent a valid alternative approach for antimicrobial discovery, as well as for the development of chemical probes to study the role of protein−protein interactions in the regulation of transcription.

METHODS

Strains and Plasmids. Bacterial strains and plasmids used in this study are listed in Table 1.

Pharmacophore Design and Compound Screening. A pharmacophore model was generated on *B. subtilis* σ^A residues utilizing data generated from mutagenesis of the RNAP β'-CH region using the "add query feature" in Accelrys Discovery Studio version 2.0 (Biovia). Hydrogen bond acceptors, hydrogen bond donors, and hydrophobes were added on the basis of the property of the amino acid residues. Each feature was defined by a central point, a location constraint sphere, and a second sphere, which signified hydrogen acceptors and

DOI: 10.1021/acsinfecdis.5b00058
ACS Infect. Dis. 2016, 2, 39−46

Table 1. Strains and Plasmids Used and Created in This Study[a]

strain	genotype	source/construction
Escherichia coli		
DH5α	F⁻ *endA1 hsdR17 supE44 thi-1 λ⁻ recA1 gyrA96 relA1* Δ*(lacZYA-argF)U169* ϕ80 d*lacZ* Δ*M15*	Gibco BRL
BL21 (DE3) pLysS	*F⁻ ompT gal dcm lon hsdS$_B$(r_B^- m_B^-) λDE3 pLysS(cm^R)*	ref 29
Bacillus subtilis		
EU168	*Prototroph*	ref 30
BS23	*trpC2 chr:: pNG24 (atpA−gfp* P_{xyl}*-'atpA cat)*	ref 21
BS1048	*trpC2 chr::pST3 (rpoC−gfp cat* P_{xyl}*-'rpoC)*	ref 22
Saccharomyces cerevisiae		
Red Star	*Prototroph*	Lesaffre, WI, USA
plasmids		
pNG209	*bla* $P_{\phi 10}$*−'6xHis -*T_ϕ	ref 25
pNG651	*bla* $P_{\phi 10}$*−3CGST-*T_ϕ	ref 14
vectors for protein overproduction		
pNG590	*bla* $P_{\phi 10}$*−6xHis−sigA-*T_ϕ	ref 15
pNG786	*bla* $P_{\phi 10}$*−rpoC*$_{(aa1-334)}$*-3CGST-*T_ϕ	ref 14
pNG871	*bla* $P_{\phi 10}$*-TFIIB*$_{(aa1-315)}$*-6xHis -*T_ϕ	this work; *TFIIB*$_{(aa1-315)}$ cloned into *Nde*I and *Acc*65I cut pNG209
pNG899	*bla* $P_{\phi 10}$*-RPB1*$_{(aa236-347)}$*-3C-GST-*T_ϕ	this work; *RPB1*$_{(aa236-347)}$ cloned into *Nde*I and *Acc*65I cut pNG651
pNG908	*bla* $P_{\phi 10}$ *−rpoC*$_{(aa220-315)}$*-PKA-3CGST-*T_ϕ	ref 14
pNG997	*bla* $P_{\phi 10}$*−6xHis−rpoD-*T_ϕ	ref 14

[a] *bla*, *cat*, ampicillin, and chloramphenicol resistance gene; $P_{\phi 10}$, phage T7 promoter; P_{xyl}, xylose inducible promoter, T_ϕ, T7 transcription terminator; 3C, the recognition sequence of 3C protease; GFP, green florescence protein; GST, glutathione *S*-transferase; PKA, protein kinase A recognition site.

donors interacting with the β′-CH region. After generation of the pharmacophore model, the protocol "search 3D database" was chosen to set up the input database as mini-Maybridge and the input pharmacophore as above, "Align ligand" set to true, "search method" set to fast, and "What to output" set to one conformation. After the results were obtained, the energy-minimized conformation of each of the compounds was generated using the software. Default parameter settings were applied, with the following exceptions: Conformation Method BEST, Maximum Conformations 255, Energy Threshold 20.0. Compounds that had to undergo a large conformational change to satisfy the pharmacophore properties were rejected. The remaining compounds were then mapped onto the RNAP β′-CH region model and default parameter settings applied, with the following exceptions: Conformation Generation NONE, Best Mapping Only TRUE, Maximum Omitted Features 1, Fitting Method RIGID. Hits where the distance of the compound to the protein was <2 Å were rejected. Compounds were purchased for testing from MolPort (Riga, Latvia), and data showing the purity of **C5** (>95%) is presented in the Supporting Information.

Protein Overproduction and Purification. Plasmids used for overproduction of protein fragments are listed in Table 1. *B. subtilis* s^A, *E. coli* s^{70}, and *B. subtilis* RNAP β′ subunit fragments with amino acid coordinates 1−334 and 220−315 were overproduced and purified as described previously.[14,25] *E. coli* BL21 (DE3) was transformed with pNG871 (TFIIB-His) or pNG899 (RPB1 CH-GST) (Table 1), and cultures were grown in autoinduction medium for 48 h at 25 °C. Following lysis and clarification, the His-tagged TFIIB fragment was purified using a 1 mL HisTrap HP column (GE Healthcare), and the GST tagged RPB1 fragment was purified using a 1 mL GSTrap column (GE Healthcare) or 1 mL of rehydrated GST−agarose resin (Sigma-Aldrich) in a gravity flow column according to the manufacturer's instructions. Purified proteins were dialyzed into 20 mM KH_2PO_4, 150 mM NaCl, 30% glycerol, pH 7.8, and stored at −80 °C.

ELISA-Based Assays. Compounds for testing were dissolved to 50 mM in DMSO and subsequently diluted in PBS for ELISA (all soluble at ≥1 mM). ELISAs were performed as described previously.[14,26] Briefly, σ^A (250 nM in PBS) was added to NUMC Maxisorp 96-well pates and incubated overnight at 4 °C. After washing, wells were blocked with 10% (w/v) BSA in PBS at room temperature for 2 h. After washing, β′-CH−GST (200 nM) was mixed with compound (500 μM) at 37 °C for 5 min before addition to the wells and incubation at room temperature for 1 h. A 1:2000 dilution of anti-GST antibody (Sigma-Aldrich) was added after washing and incubated for 1 h at room temperature. Color was developed after washing by adding 3,3′,5,5′-tetramethylbenzidine (TMB) liquid substrate system for ELISA (Sigma-Aldrich) and incubating at 37 °C with shaking at 600 rpm for 6 min prior to reading the A_{600}.

Isothermal Calorimetric Titration. ITC experiments were performed as described previously:[14] Program "plate", mode "control", reaction temperature 30 °C, 19 injections (2 μL/inj), 150 s interval between injections, stirring speed 1000 rpm. The β′-CH−GST or RPB1 CH−GST fusion (40 μM) in 50 mM KH_2PO_4, 150 mM NaCl, pH 7.4, buffers were titrated against 400 μM compound in identical buffer.

Transcription Assays. Transcription assays were performed as described previously.[14] One microliter of 1 μM *E. coli* RNAP core enzyme was mixed with **C5** (0.02−20 μM final concentration) and incubated on ice for 10 min. One microliter of 0.5 μM purified σ^{70} was then added, and the reaction mixture was made up to a final volume of 50 μL with 5 μL of 350 nM purified template DNA in DEPC water, 5 μL of 10× transcription buffer (400 mM Tris-HCl, 1.6 M KCl, 100 mM $MgCl_2$, 10 mM DTT, 50% glycerol, pH 7.9, in DEPC-treated water), 1 μL each of 10 mM ATP, GTP, and CTP, 2.5 mM UTP, 1 μL of α-^{32}P UTP (3000 Ci/mmol), and DEPC-treated

DOI: 10.1021/acsinfecdis.5b00058
ACS Infect. Dis. 2016, 2, 39−46

water. The reaction was incubated at 37 °C for 5 min. The reaction was stopped by transferring 10 μL of the reaction mixture into 5 μL of RNA gel loading buffer (95% formamide, 0.05% bromophenol blue, and 0.05% xylene cyanol), followed by heating at 95 °C for 2 min and run on a 6% denaturing polyacrylamide gel at 50 W and 50 °C in 1× TBE buffer. After drying at 60 °C for 1.5 h, the gel was imaged and relative band intensity determined using ImageJ software (NIH). To examine the competition of **C5** with σ factor in transcription, 1 μL of 1 μM core RNAP and 1 μL of 0.5 μM σ^{70} were premixed and equilibrated on ice for 10 min prior to the addition of inhibitor at 20 nM and 0.2 μM final concentration. All other steps were the same as above.

Single-round transcription assays were performed as described previously.[26,27] Briefly, 1 μL of 1 μM RNAP core enzyme was mixed with the appropriate concentration of **C5** and incubated on ice for 10 min. One microliter of 0.5 μM purified σ^{70} and 3 μL of 0.5 μM template DNA were then added and made up to 50 μL with 5 μL of 10× transcription buffer (400 mM Tris-HCl, 1.6 M KCl, 100 mM $MgCl_2$, 10 mM DTT, 50% (v/v) glycerol, pH 7.9), 1 μL each of 10 mM ATP, GTP, and CTP, 2.5 mM UTP, 1 μL of α-^{32}P UTP (3000 Ci/mmol), heparin (20 μg/mL final concentration), and H_2O. Alternatively, 1 μL of 0.5 μM purified σ^{70} was added to RNAP and incubated on ice for 10 min to form holoenzyme prior to the addition of **C5**. The reaction mixture was incubated at 37 °C for 20 min, then quenched and loaded onto gels as above.

Fluorescence Microscopy. Microscopy was performed as described previously.[21,28] *B. subtilis* strains BS23 (ATP synthase-GFP) and BS1048 (RpoC-GFP) (Table 1) were grown on nutrient agar containing 5 μg/mL chloramphenicol and 0.5% (w/v) xylose. Single colonies were picked and then incubated in LB medium supplemented with 5 μg/mL chloramphenicol and 0.5% (w/v) xylose at 37 °C until OD_{600} ~0.6. The compound or antibiotics were then added and the cultures incubated for a further 15 min. Five microliters of cell culture was placed onto 1.2% (w/v) agarose pads and a coverslip placed on top prior to imaging. A Zeiss Axioscop 2 epifluorescence microscope fitted with a CoolLED pE-4000 light source and Hamamatsu Orca II cooled CCD camera was used to capture GFP fluorescence images, which were processed using MetaMorph version 7.01 (UIC). After background subtraction, final images were assembled using Adobe Photoshop.

Antibacterial Activity Test. Fifty millimolar compound **C5** in DMSO was serially diluted in 100 μL of LB medium in the range from 3.125 to 100 μM into individual wells in a 96-well plate. *E. coli* DH5α, *S. aureus* USA300, and *B. subtilis* EU168 cells were incubated at 37 °C in 5 mL of LB until OD_{600} ~0.6, and 5 μL of the culture was added to each well. The plate was incubated in a FLUOstar Optima plate reader (BMG Labtech) at 37 °C with shaking at 600 rpm. *S. cerevisiae* Red Star was grown under identical conditions except the temperature was adjusted to 30 °C and compounds were added in the range from 31.25 to 1000 μM. The OD_{600} of each culture was taken every 10 min over an 18 h period. All assays were performed in triplicate and the growth curves compared to those of cells exposed to medium containing equivalent amounts of DMSO.

■ ASSOCIATED CONTENT

Supporting Information

The Supporting Information is available free of charge on the ACS Publications website at DOI: 10.1021/acsinfecdis.5b00058.

LC-MS and NMR analysis of **C5** (PDF)

■ AUTHOR INFORMATION

Corresponding Author

*(P.J.L.) E-mail: Peter.Lewis@newcastle.edu.au. Phone: +612 4921 5701.

Notes

The authors declare no competing financial interest.

■ ACKNOWLEDGMENTS

This work was funded by grants from the National Health and Medical Research Council (NHMRC) of Australia (G1008014; PJL) and a Faculty Early Career Award from the University of Newcastle (C.M.).

■ ABBREVIATIONS

RNAP, RNA polymerase; MRSA, methicillin-resistant *Staphylococcus aureus*; GFP, green fluorescent protein

■ REFERENCES

(1) WHO. (2014) *Antimicrobial Resistance: Global Report on Surveilance 2014*, pp 1−257, Geneva, Switzerland.
(2) O'Neill, J. (2014) *Review on Antimicrobial Resistance: Tackling a Crisis for the Health and Wealth of Nations*, HMSO, London, UK.
(3) Cramer, P. (2002) *Multisubunit RNA polymerases. Curr. Opin. Struct. Biol. 12* (1), 89−97.
(4) Sensi, P., Margalith, P., and Timbal, M. T. (1959) Rifomycin, a new antibiotic; preliminary report. *Farmaco Sci. 14* (2), 146−147.
(5) Scott, L. J. (2013) Fidaxomicin: a review of its use in patients with Clostridium difficile infection. *Drugs 73* (15), 1733−1747.
(6) Mariani, R., and Maffioli, S. I. (2009) Bacterial RNA polymerase inhibitors: an organized overview of their structure, derivatives, biological activity and current clinical development status. *Curr. Med. Chem. 16* (4), 430−454.
(7) Villain-Guillot, P., et al. (2007) Progress in targeting bacterial transcription. *Drug Discovery Today 12* (5−6), 200−208.
(8) Sonenshein, A. L., et al. (1977) Lipiarmycin-resistant ribonucleic acid polymerase mutants of *Bacillus subtilis*. *J. Bacteriol. 132* (1), 73−79.
(9) Keller, A., et al. (2014) A new subunit of RNA polymerase found in Gram positive bacteria. *J. Bacteriol. 196*, 3622−3632.
(10) Murakami, K. S., and Darst, S. A. (2003) Bacterial RNA polymerases: the whole story. *Curr. Opin. Struct. Biol. 13* (1), 31−39.
(11) Andre, E., et al. (2004) A multiwell assay to isolate compounds inhibiting the assembly of the prokaryotic RNA polymerase. *Assay Drug Dev. Technol. 2* (6), 629−635.
(12) Hinsberger, S., et al. (2013) Discovery of novel bacterial RNA polymerase inhibitors: pharmacophore-based virtual screening and hit optimization. *J. Med. Chem. 56* (21), 8332−8338.
(13) Arthur, T. M., Anthony, L. C., and Burgess, R. R. (2000) Mutational analysis of beta '260−309, a sigma 70 binding site located on *Escherichia coli* core RNA polymerase. *J. Biol. Chem. 275* (30), 23113−23119.
(14) Ma, C., et al. (2013) Inhibitors of bacterial transcription initiation complex formation. *ACS Chem. Biol. 8* (9), 1972−1980.
(15) Johnston, E. B., Lewis, P. J., and Griffith, R. (2009) The interaction of *Bacillus subtilis* sigmaA with RNA polymerase. *Protein Sci. 18* (11), 2287−2297.
(16) Bergendahl, V., Heyduk, T., and Burgess, R. R. (2003) Luminescence resonance energy transfer-based high-throughput

DOI: 10.1021/acsinfecdis.5b00058
ACS Infect. Dis. 2016, 2, 39−46

screening assay for inhibitors of essential protein-protein interactions in bacterial RNA polymerase. *Appl. Environ. Microbiol. 69* (3), 1492−1498.
(17) Glaser, B. T., et al. (2007) LRET-based HTS of a small-compound library for inhibitors of bacterial RNA polymerase. *Assay Drug Dev. Technol. 5* (6), 759−768.
(18) Lipinski, C. A., et al. (2001) Experimental and computational approaches to estimate solubility and permeability in drug discovery and development settings. *Adv. Drug Delivery Rev. 46* (1−3), 3−26.
(19) Kostrewa, D., et al. (2009) RNA polymerase II-TFIIB structure and mechanism of transcription initiation. *Nature 462* (7271), 323−330.
(20) Mooney, R. A., et al. (2009) Regulator trafficking on bacterial transcription units in vivo. *Mol. Cell 33* (1), 97−108.
(21) Johnson, A. S., van Horck, S., and Lewis, P. J. (2004) Dynamic localization of membrane proteins in Bacillus subtilis. *Microbiology 150* (Pt 9), 2815−2824.
(22) Lewis, P. J., Thaker, S. D., and Errington, J. (2000) Compartmentalization of transcription and translation in *Bacillus subtilis*. *EMBO J. 19* (4), 710−718.
(23) Dworsky, P. (1975) Unfolding of the chromosome of *Escherichia coli* after treatment with rifampicin. *Z. Allg. Mikrobiol. 15* (4), 243−247.
(24) Davies, J., and Davies, D. (2010) Origins and evolution of antibiotic resistance. *Microbiol. Mol. Biol. Rev. 74* (3), 417−433.
(25) Yang, X., and Lewis, P. J. (2008) Overproduction and purification of recombinant *Bacillus subtilis* RNA polymerase. *Protein Expression Purif. 59* (1), 86−93.
(26) Yang, X., Ma, C., and Lewis, P. J. (2015) Identification of inhibitors of bacterial RNA polymerase. *Methods 86*, 45−50.
(27) Artsimovitch, I., and Henkin, T. M. (2009) In vitro approaches to analysis of transcription termination. *Methods 47* (1), 37−43.
(28) Doherty, G. P., et al. (2010) Small subunits of RNA polymerase: localization, levels and implications for core enzyme composition. *Microbiology 156* (Pt 12), 3532−3543.
(29) Studier, F. W., and Moffatt, B. A. (1986) Use of bacteriophage T7 RNA polymerase to direct selective high-level expression of cloned genes. *J. Mol. Biol. 189* (1), 113−130.
(30) Buescher, J. M., et al. (2012) Global network reorganization during dynamic adaptations of *Bacillus subtilis* metabolism. *Science 335* (6072), 1099−1103.

DOI: 10.1021/acsinfecdis.5b00058
ACS Infect. Dis. 2016, 2, 39−46